arXiv:cond-mat/0607143v1 [cond-mat.supr-con] 5 Jul 2006

A Simple Model for Thermomagnetic Instability of Critical State Dynamics in Superconductive Films

Yu. E. Kuzovlev*
Donetsk Physics and Technology Institute of NASU, 83114 Donetsk, Ukraine

An one-dimensional model of magnetic flux penetration into thin strip-like superconductive film is subject to numerical analysis, which combines explicit account for specific oblate geometry of magnetic field lines around the film and a simplest phenomenology of the flux flow resistance under rigid pinning of vortices with temperature-dependent critical current.

PACS numbers: 74.78.-w, 74.25.Fy, 74.25.Op, 74.25.Qt

1. During last decade, the classical theory of thermomagnetic instability of excited critical states in type II superconductors [1] was supplemented with new numeric models and simulations [2, 3] and new theory beyond them [4, 5, 6]. Both well explain the complicated dendritic fragmentation of magnetic flux observed experimentally [7]. Especially impressive are simulations in terms of "atoms" with long-range interactions specific for vortices in films [2] (see also references and pictures at http://www.fys.uio.no).

It seems interesting to compare so advanced "microscopic" approach with primitive "hydrodynamical" models. Below we consider, perhaps, most simple one: an 1-D model of magnetic flux penetration into strip with strong pinning of vortices. Our main issue will be explicit account for effects of real film's geometry, which involve non-uniformity of interaction between vortices, that is its long-range dependence on their absolute, in addition to relative, positions. Note that such non-uniformity may be inessential in respect to fine structure of captured magnetic flux (visualized by magneto-optics [2, 7]) but essential in respect to its global characteristics (measured with SQUID or pickup coil [7, 8]).

2. A simple variant of the classical theory [1] reduces to equations (in CGS units)

$$\frac{\partial \boldsymbol{B}}{\partial t} = -\,c\nabla\times\boldsymbol{E}\ ,\quad J=\frac{c}{4\pi}\,\nabla\times\boldsymbol{B}\ , \tag{1}$$

$$\boldsymbol{E}=\boldsymbol{E}(\boldsymbol{J},\boldsymbol{B},T)\ ,\quad \frac{\partial T}{\partial t}=\ldots+\frac{\boldsymbol{J}\cdot\boldsymbol{E}}{C}\ , \tag{2}$$

with magnetic inductance $\boldsymbol{B}$, electric field $\boldsymbol{E}$, electric current density $\boldsymbol{J}$, temperature T, velocity of light c, specific heat C, "constitutive law" $\boldsymbol{E}=\boldsymbol{E}(\boldsymbol{J},\boldsymbol{B},T)$ resulting from viscous dynamics of vortices and their pinning, and the dots deputizing for heat transfer.

In case of superconductive film, one also needs in the Laplace equation for magnetic field out of film, in order to state a relation between tangential and normal components of the field at film's surface. At present, analytical solutions to this problem are known for two film shapes only: strip [9, 10] and disk [11, 12]. The first case is simpler, therefore let our film will be a strip oriented along Y-axis, with section $|X|<L/2$, $|Z|<d/2$, where L and d are film's width and thickness, respectively.

Firstly, let us transform Eqs.1-2 into dimensionless form, choosing $x_0=L/2$ to be unit of length (then the section becomes $|X|<1$, $|Z|<\delta\equiv d/L$), $t_0=x_0H_{c2}/c\rho_nJ_c$ as unit of time, with H_{c2} being upper critical field, ρ_n - characteristic normal specific resistance, and J_c - maximum critical current density, $j_0=J_c$ as unit of current density, $b_0=2\pi dJ_c/c$ as unit of magnetic field, and $e_0=b_0x_0/ct_0$ as unit of electric field.

Secondly, carry through spatial averaging of $\boldsymbol{B}$, $\boldsymbol{J}$ and other patterns along strip length, designating this operation by $\langle\ldots\rangle_Y$, and introduce the quantity

$$I(x,t)\ =\ \frac{2\pi}{c}\left\langle\int_{-d/2}^{d/2}J_y(x,y,z,t)\,dz\right\rangle_Y \tag{3}$$

Applying $\langle\ldots\rangle_Y$ to Eqs.1 and using the Clem et al. [9] and Brandt results [10] it easy to obtain

$$\frac{\partial B}{\partial t}=-\,\frac{\partial E}{\partial x}\ , \tag{4}$$

$$I(x,t)\ =\int_{-1}^{1}\sqrt{\frac{1-u^2}{1-x^2}}\ \frac{B(u,t)-H_0(t)}{\pi\,(x-u)}\,du\ , \tag{5}$$

where $B=B(x,t)$ is normal component of $\langle\boldsymbol{B}\rangle_Y$ additionally averaged over thickness of the film, $E=E(x,t)$ is similarly twice averaged Y-component of $\boldsymbol{E}$, and H_0 is external bias field (assumed uniform and perpendicular to film). The Eqs.4 and 5 are applicable irrespective of any "dendritic" or other longitudinal non-uniformities, if only $\boldsymbol{B}$ possesses statistical uniformity.

The integral in (5) is nothing but exact average tangential component of $\boldsymbol{B}$ at upper film's surface in the formal limit $\delta\to 0$. At that, we will keep in mind that physically our film is "not too thin": $d>\lambda$ with λ being characteristic penetration depth. This allows to interpret magnetic flux density $B(x,t)$ as direct measure of concentration of vortices.

What is for the averaging of the "constitutive law", $\boldsymbol{E}=\boldsymbol{E}(\boldsymbol{J},\boldsymbol{B},T)$, it is less trivial, since its result, some

*Electronic address: kuzovlev@kinetic.ac.donetsk.ua

effective law $E = E(I, B, T)$ for averaged variables, can be sensible to any non-uniformities. At present, lacking something better, we will try something from traditional model laws. For instance (in our dimensionless units),

$$E(I, B, T) \;=\; \rho(B)\, I_n(I, T)\;, \tag{6}$$

$$I_n(I,T) = \left\{ \begin{array}{lll} I - I_c(T) & , & I > I_c(T) \\ 0 & , & |I| < I_c(T) \\ I + I_c(T) & , & I < -I_c(T) \end{array} \right. , \tag{7}$$

$$\rho(B) = |B|\;, \quad I_c(T) = 1 - Q\;, \quad Q \equiv \frac{T - T_0}{T_c - T_0} \tag{8}$$

Here $\rho(B)$ represents the "flux flow resistance", I_c is critical value of I as a function of local temperature, and T_0 and T_c are background (thermostat) and critical temperature, respectively.

Thus the model assumes "rigid" pinning without creep, when vortices can move under $|I| > I_c(T)$ only. At that, the excess current $I_n = I_n(I, T)$ directly determines local drift velocity of vortices while the electric field $E = |B| I_n$ local flux flow. Frequently I_n is treated conversely as "normal current" caused by motion of vortices. But we will see below that sometimes I_n turns into Meissner super-current shielding a part of film. In such "quasi-Meissner" states, in addition to drift of vortices, their diffusion may be important. We will take it into account if replace Eq. 4 by

$$\frac{\partial B}{\partial t} \;=\; -\,\frac{\partial}{\partial x}\,|B| I_n(I,T) \;+\; \frac{\partial}{\partial x}\,\Delta(I,T)\frac{\partial B}{\partial x}\;\;, \tag{9}$$

$$\Delta(I,T) \;=\; \left\{ \begin{array}{lll} 0 & , & |I| < I_c(T)\;, \\ \Delta & , & |I| > I_c(T)\;, \end{array} \right. \tag{10}$$

so that diffusion occurs only when vortices get free from pinning. In view of the Einstein relation, the diffusivity Δ is definite function of the foregoing parameters. In our dimensionless units, $\Delta = 2T/f_c L$, with $f_c \equiv \Phi_0 J_c d/c$ being characteristic critical Lorentz force and pinning force acting per vortex.

Boundary conditions to the diffusive term in Eq.9 will state continuity of average normal component B_z of magnetic inductance at film's edges $x = \pm 1$. Outside of the strip it can be obtained from (see [9])

$$B_z = H_0 + \mathrm{Im} \int_{-1}^{1} \sqrt{\frac{1-u^2}{1-w^2}}\;\frac{B(u) - H_0}{\pi\,(u-w)}\,du \tag{11}$$

where $w \equiv x + i|z|$, time is omitted, and $B_z \equiv \langle B_z(x,y,z)\rangle_Y$. Particularly, in film's plane (at $|x| > 1$)

$$B_z(x,0) \;= H_0 - \int_{-1}^{1} \sqrt{\frac{1-u^2}{x^2-1}}\;\frac{B(u) - H_0}{\pi\,|u-x|}\,du \tag{12}$$

At very edges, of course, factor $1/\sqrt{x^2-1}$ should be reasonably cut, e.g. by $1/\sqrt{2\delta}$.

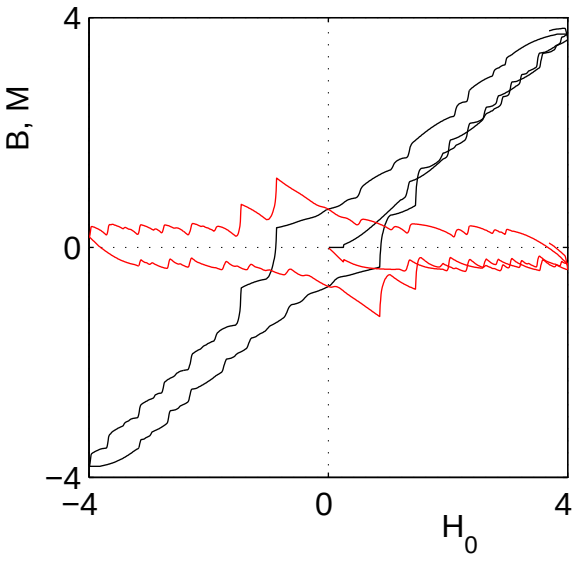

FIG. 1: Hysteresis loops of mean magnetic inductance, $\overline{B}(t) = \int B(x,t)\,dx\,/L$ (black), and magnetization, $M(t) = \overline{B}(t) - H_0(t)$ (red), after start from ZFC (zero field cooled) state under saw-like $H_0(t)$ with period 200, at parameters $p = 10$, $\gamma = 2$ and $D = 0.03$.

To finish writing of the temperature equation, include there heat diffusion across film and local heat exchange among it and its substrate. In the dimensionless form,

$$\frac{\partial Q}{\partial t} = D\frac{\partial^2 Q}{\partial x^2} - \gamma Q + p\,IE(I,B,T)\;, \tag{13}$$

$$p \;\equiv\; 2\pi L d J_c^2/[c^2(T_c - T_0)C] \tag{14}$$

(for simplicity, C and D assumed temperature independent). Estimates of dimensionless thermal diffusivity, thermal relaxation rate, Joule heating and vortex diffusivity for realistic films typically yield $D \sim 0.01$, $\gamma \sim 1$, $p \sim 10$, and $\Delta \sim 10^{-8}$ (although values $10 \div 100$ times greater or smaller also may be realistic).

3. The system of equations (5)-(13) was numerically investigated using the third-order adaptive Runge-Kutta algorithm. The integral in (5) was reduced to the Hilbert transform (at finite interval) in its turn performed through fast Fourier transform. It was found that subject to values of p/γ and $|dH_0(t)/dt|$ the model has rich variety of regular and chaotic regimes of magnetic flux entry into film or departure from it. But we will not list all that. Our aim is to list only main properties of the system manifested in all regimes, and illustrate them by intermediate quasi-regular regimes with $p/\gamma \sim 10$ and $dH_0(t)/dt \sim \pm 0.1$.

Fig.1 demonstrates clear signs of many magnetic flux avalanches with different magnitudes and durations. Relatively large-scale and reproducible avalanches alternate with quiet flux creep which on closer examination consists of many small-scale avalanches. Most tiny of them

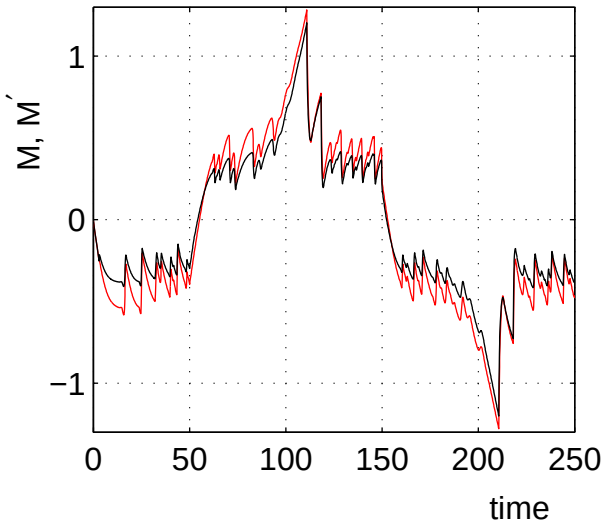

FIG. 2: Two variants of total film's magnetization, $M = \overline{B} - H_0$ (black) and M' introduced by Eqs.15-16 (red), via time, under the same conditions as in Fig.1.

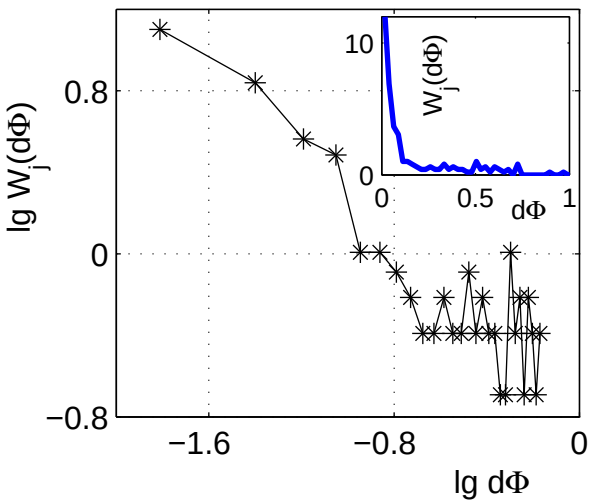

FIG. 3: Histogram of magnetic flux jumps determined from "horizontal inflections" of $\overline{B}(t)$ (see body text), under the same conditions as in Figs.1-2, in double logarithmic and (inset) linear scales.

are indistinguishable from random computational errors which thus serve as mathematical noise generator imitating physical thermal fluctuations. Under the adaptive algorithm, a level of this noise occurs rather constant.

From thermodynamical point of view, the mean flux density $\overline{B} = \int_{-L/2}^{L/2} B(x,t)\,dx/L$ and corresponding magnetization $M = \overline{B} - H_0$ shown in Fig.1 seem most natural global magnetic characteristics of the film. But, according to (11), from the point of view of any pickup coil the film is presented by a modified magnetization,

$$M' = \int_{-L/2}^{L/2} W(x)\,[B(x,t) - H_0]\,dx\ , \qquad (15)$$

with $W(x)$ being some weight function (normalized to unit). In particular, if a coil is placed far from film, then

$$W(x) = \frac{2}{\pi}\sqrt{1-x^2} \qquad (16)$$

(in the dimensionless form). Fig.2 shows time evolvent of such defined M' in comparison with M.

It is popular to search for scale invariance in size distributions of the avalanches. Then one firstly should introduce a criterion for their beginnings and endings. For example, let us define the borders between subsequent flux jumps as those inflection points of the plot $\overline{B}(t)$ where $|d\overline{B}(t)/dt|$ has local minimums, and interpret increments or decrements of $\overline{B}(t)$ between these points (after multiplying them by film's width) as heights $d\Phi$ of the jumps. Their probability density $W_j(d\Phi)$ (normalized histogram) is shown in Fig.3. By request, one can find here good signs of the scaling. But dominant smooth part of this probability density corresponds to mini-avalanches invisible in Figs.1 and 2.

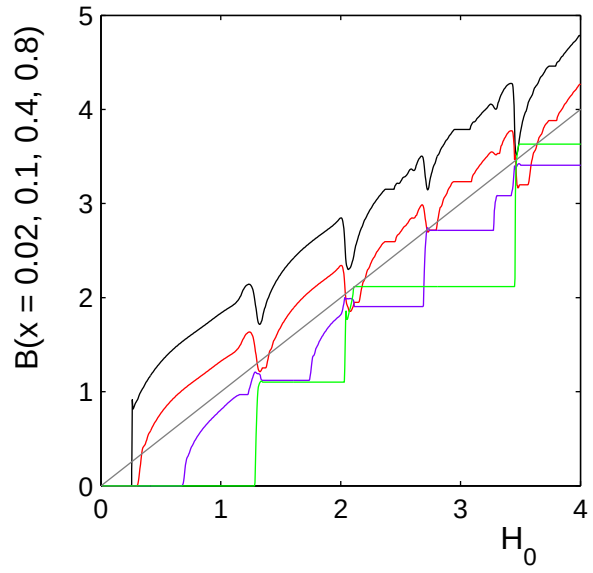

FIG. 4: Magnetic inductance at $x = 0.02$ (black), $x = 0.1$ (red), $x = 0.4$ (blue) and $x = 0.8$ (green), as a function of external field rising linearly from ZFC state ($H_0(t) = 0.08t$). The gray straight line guides $B = H_0$, and x means distance from left film's edge.

4. Consider peculiarities of the model which are definitely caused by its flat thin-film geometry.

First, even in simplest situation, when external field slowly and monotonously (linearly) goes up from ZFC state, local magnetic flux density inside film can be strongly non-monotone function of both time and position. Second, in some vicinity of film's edges the flux density can significantly exceed external field. The latter circumstance as well as the temporal non-monotony are

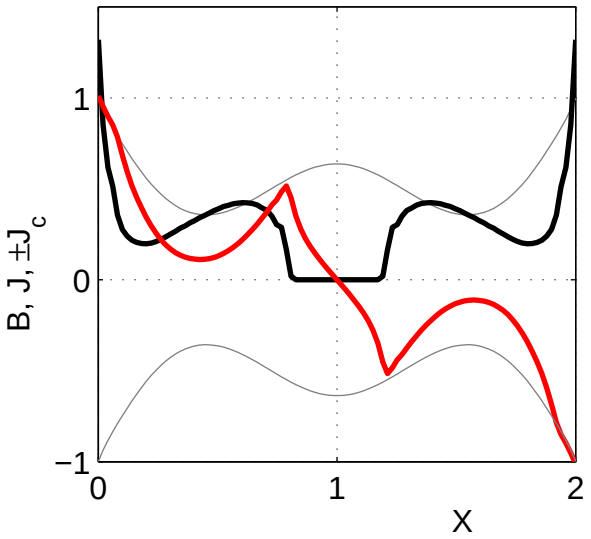

FIG. 5: Typical instant spatial distributions of magnetic flux density $B(x,t)$ (black), current $I(x,t)$ (red) and critical current $\pm I_c(x,t)$ (gray) across strip's width, at beginning stage of the process shown in Fig.4. As in Fig.4, x is dimensionless coordinate counted from left film's edge.

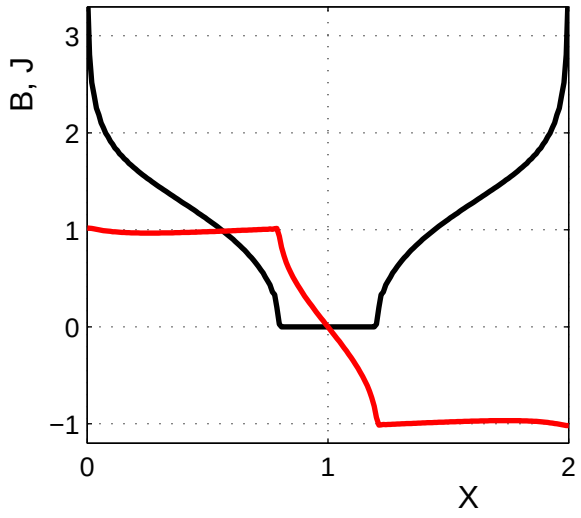

FIG. 6: Spatial distributions of magnetic flux density $B(x,t)$ (black) and current $I(x,t)$ (red) under linearly rising external field in absence of thermomagnetic instability ($p/\gamma \ll 1$).

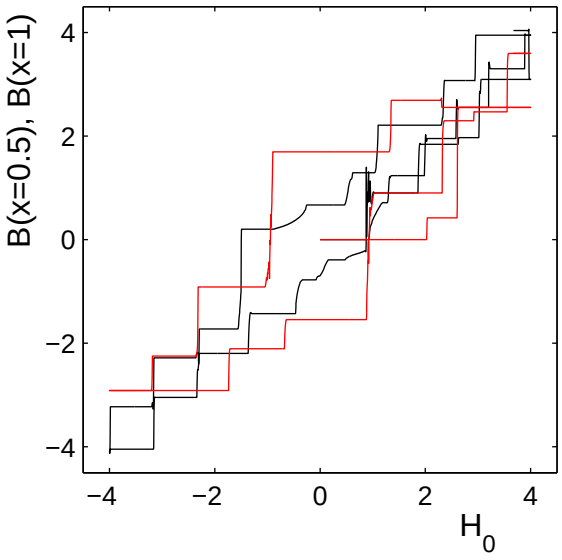

FIG. 7: Local flux density in the middle part of the film at $x = 0.5$ (black) and in its center at $x = 1$ (red) under the same conditions as in Fig.1, with x being distance from left film's edge.

demonstrated at Fig.4 (in fact it relates to initial stage of the same process as in Figs.1-3).

Of course, the reason for such behavior is strong compression of magnetic field lines near film's edges (formally, at $\delta \to 0$ magnetic inductance at very edges can be arbitrary large). Sufficiently big avalanche drops the compression down, but then pinning enforces it to grow again.

Example of spatial non-monotony is presented in Fig.5. This snapshot is made just after avalanching. It is seen that the current became smaller then critical current and thus flux motion is stopped everywhere except the film's periphery, where slow creep (formed by local mini-avalanches) takes place. Note that in accordance with (8) corresponding temperature pattern can be viewed if lift the lower gray curve $-I_c(x)$ by unit.

Clearly, such picture of $B(x)$ as in Fig.5 never could be observed (in similar process) under 3-D cylindric geometry, since non-monotony of $B(x)$ would mean sign reversal of $J(x) \propto -\partial B(x)/\partial x$ and thus reverse flux flow. But under film geometry, when differential relation between magnetic inductance and current changes into integral relation (5), the $B(x)$'s non-monotony does not necessarily involve $I(x)$'s sign reversal. Consequently, 2-D geometry produces much more intricate patterns.

For comparison, Fig.6 shows what the model gives when thermomagnetic instability is out of play, under $p/\gamma \ll 1$. Then penetration of magnetic flux realizes merely as smooth drift, additionally stimulated by weak diffusion and noise when $H_0(t)$ crosses zero (see below). At that, instant $B(x,t)$'s and $I(x,t)$'s patterns almost do not differ from ones at static critical state under the same but fixed external field.

One more interesting thing seen from Fig.4 is discretization of local flux density values deep in the film. Hysteresis loops drawn by them are shown in Fig.7. These pictures prove that almost all avalanches begin at periphery of the film and therefore flux filling of its interior comes from most powerful avalanches, while smaller ones never reach its middle.

The evident presence of a large amount of randomness (partly chaos and partly noise) in evolution of $B(x,t)$ and $I(x,t)$ distributions inevitably results in breakdown of mirror symmetry of $B(x,t)$ and anti-symmetry of $I(x,t)$, which is illustrated by Fig.8. The breakdown oc-

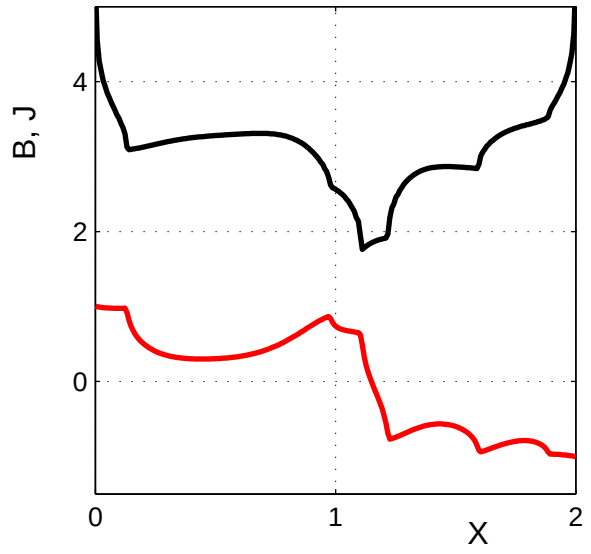

FIG. 8:
Typical picture of the mirror symmetry breakdown, photographed at time 42.5 (when $H_0 = 3.4$) during the same process as in Fig.1 and Fig.2.

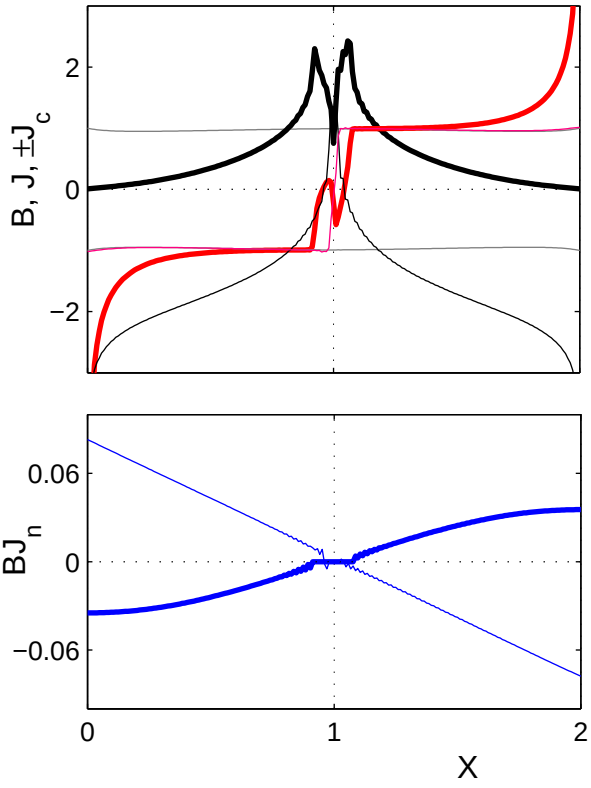

FIG. 9:
Top: Patterns of magnetic flux density $B(x,t)$ (black) and current $I(x,t)$ (red) during quasi-Meissner state before explosive flux reversal (thick curves) and quasi-critical state after it (thin curves). The gray lines show $\pm I_c$.
Bottom: Distributions of flux flow BI_n in the two above mentioned situations. For details see body text.

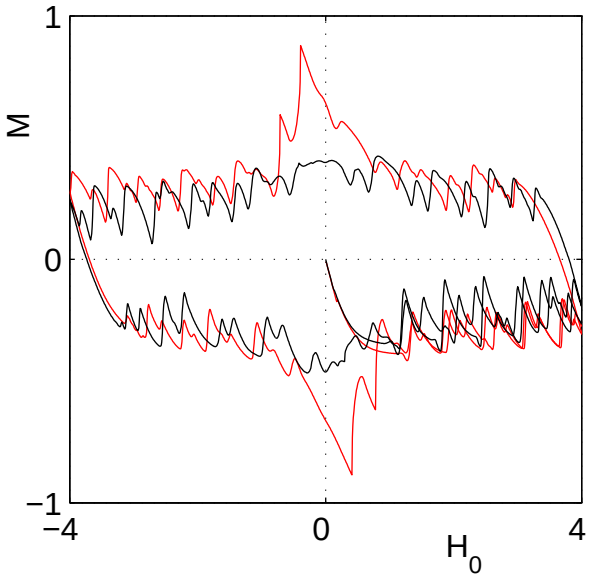

FIG. 10: Hysteresis loops of magnetization under the same parameters as in Figs.1-2 but with 30 times greater (red curve) and 1000 times greater (black curve) Δ value.

curs soon after start from ZFC and then never completely disappears, although the symmetry partly restores at borders between quadrants of the $H_0 - M$ diagram.

5. Next, we focus our attention on two (mutually inverse) biggest peaks of the magnetization in Figs.1 and 2 (at time moments $t \approx 110$ and $t \approx 210$) and also on red curve in Fig.10. They represent not usual avalanches but flux reversal in the film when $H_0(t)$ passes through zero. This process is illustrated also by Fig.9.

At that time (if saying about positive peak) earlier accumulated positive magnetic flux decreases down to zero and then changes its sign. This realizes in two different ways: at first by flow of positive flux out of film, when vortices leave it, and afterwards by flow of negative flux into film, when anti-vortices enter it and annihilate with vortices in its interior. Obviously, transition from the "vortex departure stage" to the "anti-vortex entry stage" occurs when (i) magnetic field B_z^{edge} at outward vicinity of film's edges becomes negative and then (ii) diffusive flow of anti-vortices at film edges, F_{av}, becomes exceeding drift outflow of vortices, $F_v = B(x = \pm 1)I_n(x = \pm 1)$ (importantly, anti-vortices do not contribute to drift because their concentration is zero while the first "departure stage" still lasts).

According to Eq.12 (with the remark under it),

$$B_z^{edge} \approx H_0 - \frac{1}{\pi\sqrt{2\delta}} \int_{-1}^{1} \sqrt{\frac{1 \pm x}{1 \mp x}}\, [B(x) - H_0]\, dx \quad (17)$$

where upper sign corresponds to right-hand edge. This expression clearly implies that B_z^{edge} crosses zero before $H_0(t)$ does it. The diffusive anti-flux flow is proportional to gradient of Z-component of magnetic inductance at

the very edges and can be written as

$$F_{av} \approx \Delta\,[B(x=\pm 1) - B_z^{edge}]/\delta \ , \qquad (18)$$

by definitions of the appearing quantities (all smoothed over film thickness). The Eqs.17 and 18 lead to estimate

$$|F_{av}| \approx \frac{\Delta}{\delta^{3/2}} \left[|H_0| + \int_{-1}^{1} \sqrt{\frac{1\pm x}{1\mp x}}\, B(x)\, \frac{dx}{\pi\sqrt{2}} \right] \qquad (19)$$

valid when $H_0(t)$ already crossed zero, at $H_0 < 0$ (of course, if the transition not yet happened, and $B(x)$ looks as in Fig.9).

Hence, at sufficiently small $\Delta/\delta^{3/2}$ the transition from "departure stage" to "entry stage" can be strongly delayed. Just such example is presented by Figs.1-2, where the annihilation switches on at $t \approx 110$ only, when $H_0 \approx -0.8$ (i.e. under H_0 comparable with full penetration field!).

This results in strong"supersaturation" of the vortex system and, as consequence, fast explosive transition, which manifests itself in Figs.1-2 as high sharp steep in $\overline{B}(t)$ and $M(t)$ plots. Increase of Δ, under the same thickness, shortens "departure stage" but prolongs and softens "entry stage". Correspondingly, the steep in magnetization curve decreases and at sufficiently large Δ it disappears at all, as Fig.10 shows.

Of special interest is spatial structure of the departure stage. As top of Fig.9 shows, due to the outflow of vortices their peripheral concentration drops to very small values. However, the outflow continues. Therefore, $E = |B|I_n$ must be approximately independent on spatial coordinate X. Indeed, thick blue curve at bottom of Fig.9 confirms good satisfaction of this requirement, while thick red curve at top of Fig.9 shows that it is satisfied owing to strong growth of "normal current" I_n close to film's edges. There $|I_n| \sim I_c$ or even $|I_n| \gg I_c$, and this current well screens film's periphery. Hence, we see something like Meissner super-current and Meissner state!

In essence, of course, this "quasi-Meissner" state represents not a quasi-static state as true Meissner states, but sooner quasi-stationary dissipative structure, just because it is maintained by motion of vortices (up to a moment when it will be destroyed by birth of anti-vortices). In this sense, I_n by right can be qualified as dissipative "normal" current.

Thin curves at Fig.9 present distributions of $B(x,t)$ and $I(x,t)$ just after the explosive annihilation and flux reversal. Evidently, annihilation still not finished at film's center, but in the rest of film $|I| \approx I_c \approx 1$, i.e. negative flux evenly fills it. Corresponding plot of flux flow $E = |B|I_n$ is shown by thin curve at bottom of Fig.9 (we plot BI_n instead of $|B|I_n$ in order to underline transition from vortex flow to anti-vortex one). Thus, we observe typical "quasi-critical" state (but next avalanches are not far off).

6. To resume, we tested a simple model of magnetic flux penetration into films of type II superconductor with temperature-sensible pinning. Advantage of the model is that it is based on exact extremely non-local relations between flux density distribution and current distribution in film. Defects of the model are in rather rough phenomenology of dissipative and thermal processes. The constituents of the model are not original, but, to the best of my knowledge, the model as a whole still was not under careful investigation. I tried to demonstrate that it is enough substantial and interesting and even can produce useful tips for understanding experimental data.

I am very grateful to Dr. Yu. Medvedev and Dr. V. Khokhlov for fruitful information and attracting my attention to the subject of this paper.

[1] R. G. Mintz and A. L .Rakhmanov, Rev. Mod. Phys. **53**, 551 (1981).

[2] T. H. Johansen, M. Baziljevich, D. V. Shantsev, et al., Europhys. Lett. **59** (4), 599 (2002).

[3] A. L. Rakhmanov, D. V. Shantsev, G. M. Galperin, and T. H. Johansen, cond-mat/0405446.

[4] B. Biehler, B.-U. Runge, P. Leiderer and R. G. Mints, cond-mat/0410030.

[5] V. V. Chabanenko, A. I. Dyachenko, M. V. Zalutskii, et al., J. Appl. Phys. **88** (10), 5875 (2000).

[6] I. Aranson, A. Gurevich, and V. Vinokur, cond-mat/0106353.

[7] E. Altshuler and T. H. Johansen, Rev. Mod. Phys. **76**, 471 (2004).

[8] P. N. Mikheenko and Yu. E. Kuzovlev, Physica **C204**, 229 (1993).

[9] J. R. Clem, R. P. Huebener, and D. E. Gallus, J. Low. Temp. Phys. **12**, 449 (1973).

[10] E. H. Brandt, Phys. Rev. **B46**, 8628 (1992).

[11] Yu. E. Kuzovlev, cond-mat/0504320.

[12] Yu. E. Kuzovlev, cond-mat/0606368.